Formation mechanism and luminescence appearance of Mn-doped zinc silicate particles synthesized in supercritical water

Masafumi Takesue [a,b], Atsuko Suino [c], Yukiya Hakuta [c], Hiromichi Hayashi [c], Richard Lee Smith Jr. [a,*]

[a] Research Center of Supercritical Fluid Technology, Tohoku University, 6-6-11, Aramaki Aza Aoba, Aoba-ku, Sendai 980-8579, Japan
[b] Research and Development Center, Bando Chemical Industries, Ltd., 4-6-6, Minatojima Minamimachi, Chuo-ku, Kobe 650-0047, Japan
[c] Research Center for Compact Chemical Process, National Institute of Advanced Industrial Science and Technology, 4-2-1, Nigatake, Miyagino-ku, Sendai 983-8551, Japan

ARTICLE INFO

ABSTRACT

Luminescence appearance of Mn-doped zinc silicate ($Zn_2SiO_4:Mn^{2+}$, ZSM) formed in supercritical water at $400\,°C$ and $29\,MPa$ at reaction times from 1 to $4320\,min$ was studied in the relation to its phase formation mechanism. Appearance of luminescent ZSM from green emission by α-ZSM and yellow emission by β-ZSM occurred over the same time period during the onset of phase formation at a reaction time of $2\,min$. Luminescence appeared at a much lower temperature and at shorter reaction times than the conventional solid-state reaction. Needle-like-shaped α-ZSM was the most stable particle shape and phase in the supercritical water reaction environment and particles formed via two routes: a homogenous nucleation route and a heterogenous route that involves solid-state diffusion and recrystallization.

1. Introduction

Processing technologies for materials, especially those using supercritical water and hydrothermal conditions have been investigated extensively for inorganic materials containing phosphors [1–3]. Such hydrothermal processes have mainly attracted the attention of researchers aimed at producing nanoparticles. However, hydrothermal reactions in supercritical water have the potential for producing highly crystalline inorganic materials.

Presently, commercial inorganic phosphors are synthesized by conventional solid-state reaction processes [4]. In the solid-state reaction, phase formation of phosphors proceeds by solid-state diffusion among solid starting materials, whose diffusion rates are very low. Therefore, commercial inorganic phosphors are usually synthesized at reaction temperatures higher than $1000\,°C$ and for reaction times of several hours or more to produce phosphors that have high crystallinity and high luminescence. On the other hand, synthesis at supercritical conditions has the potential to obtain highly crystalline and highly luminescent phosphors at lower temperatures and shorter times than those used in the solid-state

reaction process, since reaction rates tend to be greatly accelerated in supercritical water and the solvent properties such as density of water can be varied with temperature or pressure. A low-temperature process (ca. $400\,°C$) that could overcome the limitations of solid-state diffusion would bring a large benefit to industry and help to solve both environmental and energy problems. Even though the conventional hydrothermal process can provide a low-temperature route to produce commercial phosphor, however, it is not being used on a practical scale, most likely due to the low crystallinity and therefore the low luminescence of the formed materials. In this respect, it is especially important to understand the phase formation mechanism and crystal structure for achieving highly luminescent phosphors in water at high temperatures and high pressures.

Mn-doped zinc silicate ($Zn_2SiO_4:Mn^{2+}$, ZSM) is a green emitting phosphor excited by electron beam or ultraviolet light [4,5] and has been in practical use since the 1930s, where it is used in most advanced plasma displays [4,6,7]. Zinc silicates have potential as materials for multi-color emitting phosphors by changing the dopant ion, for example, red emission by Eu^{3+} [8–11], blue emission by Eu^{2+} [12] and Ce^{3+} [13], and an additional green emission by Tb^{3+} [13,14]. ZSM and zinc silicates have received considerable attention not only as phosphor materials, but also as typical materials in processing research by a variety of methods [4,6,15–17]. Although, synthesis of ZSM has been widely studied with hydrothermal [5,18–23], and solvothermal [24] processing, the luminescence of ZSM produced by these methods

is much lower than that produced by solid-state reactions [20]. Therefore, it can be said that the phase formation mechanism of ZSM under hydrothermal conditions is still not understood well in the relationship with the luminescent properties, and further investigation is necessary to produce luminescent materials that have high crystallinity on a practical scale.

We previously studied the dissolution behavior of ZSM precursors and particle formation of ZSM in supercritical water by *in situ* observations with a hydrothermal diamond anvil cell (HDAC). In that work, we found that needle-like-shaped ZSM formed thorough homogeneous nucleation in water close to the critical point of water [25]. In this work, we examine the time evolution of the luminescence appearance and relate this to the phase formation mechanism.

2. Experimental

2.1. Materials and precursor preparation

Zinc oxalate dihydrate ($ZnC_2O_4 \cdot 2H_2O$, Kojundo Chemical Laboratory, 99.9%), manganese oxalate (MnC_2O_4, Kojundo Chemical Laboratory, 99.9%), and spherical silica particles (amorphous SiO_2, Nippon Shokubai KE-P50, mean particle diameter, 500 nm) were used as raw materials. Net SiO_2 content in the silica particles was 84.9 wt% as determined by measuring weight loss with thermogravimetric analysis. The water used was deionized water. Precursors were prepared by adequately mixing raw materials for about 30 min with an agate mortar and an agate pestle, where the Zn/Mn/Si molar ratio was 1.96/0.04/1 and thus the Mn content was 2 mol% in all experiments.

2.2. ZSM preparation in supercritical water

ZSM was produced at supercritical conditions with batch reactors made of stainless steel SUS 316 (10 mL volume). Reactions were carried out at conditions to give theoretical concentrations of ZSM of 0.075–0.60 mol/kg. Water density in the batch reactor was 0.3 g/cm³ to give a calculated pressure of 29 MPa at the reaction temperature of 400 °C. Methods for the calculation of pressure are given in the literature [26,27]. The batch reactors were heated in a molten salt bath at the given temperature (400 °C) and time (1–4320 min) and quenched in water at room temperature. Temperature inside the batch reactor was measured by a K-type thermocouple inserted into the reactor. Heat-up time required was roughly between 50 s (374 °C) and 120 s (400 °C) to reach the desired temperature with a molten salt bath. After cooling and opening the reactor, solid product was separated from the liquid by filtering with 0.1 μm membrane filters and washed several times with deionized water. The product was dried for 24 h at 60 °C in an electric oven.
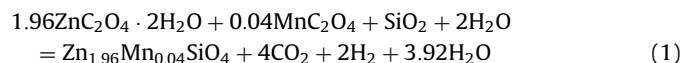
2.3. Analyses

The crystalline phase was characterized by the X-ray powder diffractometry (XRD) patterns using a Rigaku RINT2000 equipped with graphite monochromatized Cu$K\alpha$ radiation. The morphology was evaluated with scanning electron microscopy (SEM), using a JEOL JSM-5600LV at an accelerating voltage of 15–20 keV. Vacuum ultraviolet photoluminescence (VUV-PL) emission spectra were measured in a vacuum chamber equipped with a rotary pump at pressure of about 7 Pa and at room temperature. Product materials were placed into round shaped holders whose diameter was 26 mm and depth was 0.2 mm and were irradiated in a vertical orientation with a deuterium lamp, Hamamatsu Photonics L8998

(peak wavelength of emission, 161 nm) and power supply, Hamamatsu Photonics C9598. Emission was detected at a direction 45° to that of the sample with optical fibers and a photonic multichannel analyzer, Hamamatsu Photonics PMA-11. The color coordinates were calculated by using spectra observed from 380 to 780 nm and the CIE (Commission Internationale de l'Eclairage) 1931 standard colorimetric observer data (visual angle, 2°). Weight losses were measured with thermogravimetric analysis (TGA), using a Bruker AXS TG-DTA 2010SA at a heating rate of 10 °C/min to 1000 °C in N_2 atmosphere (100 mL/min). The products were dissolved in 1 M nitric acid. The elemental contents were measured with inductively coupled plasma atomic emission spectrometry (ICP-AES) (Seiko instruments SPS7800).
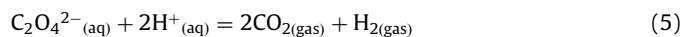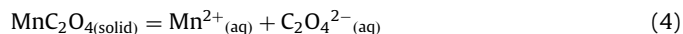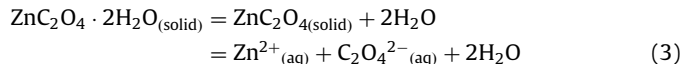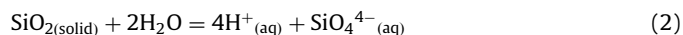
3. Results and discussion

3.1. Phase formation mechanism of Mn-doped zinc silicate in supercritical water

Analysis of products at various conditions is summarized in Table 1. The precursor is expected to react theoretically as follows:

$$1.96ZnC_2O_4 \cdot 2H_2O + 0.04MnC_2O_4 + SiO_2 + 2H_2O$$
$$= Zn_{1.96}Mn_{0.04}SiO_4 + 4CO_2 + 2H_2 + 3.92H_2O \quad (1)$$

The elementary process in reaction (1) can be expressed by Eqs. (2)–(5) as follows, assuming ionization to some extent of each of the starting materials:

$$SiO_{2(solid)} + 2H_2O = 4H^+_{(aq)} + SiO_4^{4-}_{(aq)} \quad (2)$$

$$ZnC_2O_4 \cdot 2H_2O_{(solid)} = ZnC_2O_{4(solid)} + 2H_2O$$
$$= Zn^{2+}_{(aq)} + C_2O_4^{2-}_{(aq)} + 2H_2O \quad (3)$$

$$MnC_2O_{4(solid)} = Mn^{2+}_{(aq)} + C_2O_4^{2-}_{(aq)} \quad (4)$$

$$C_2O_4^{2-}_{(aq)} + 2H^+_{(aq)} = 2CO_{2(gas)} + H_{2(gas)} \quad (5)$$

Yields were calculated by dividing experimental yields by theoretical yields assuming that Zn and Mn ions underwent conversion as $(Zn,Mn)_2SiO_4$. Theoretical mass of ZSM material that can be obtained from 100 mg of precursor is 49.8 mg.

The color of all products was white by visual examination in white light. Yields for reaction times below 5 min were over 100% because unreacted starting materials remained in the samples. These samples also showed large weight losses during TG-DTA measurements. For the product obtained at a reaction time of

Table 1
Analysis of Mn-doped zinc silicate produced by supercritical process

Run no.	Concentration of ZSM (mol/kg)	Reaction time (min)	Yield (%)	Weight loss (wt%)	Mn content (mol%)
1	0.30	1	172.3	43.5	2.1
2	0.30	2	154.6	43.1	1.7
3	0.30	3	130.4	29.1	1.4
4	0.30	4	121.7	25.1	1.6
5	0.30	5	109.7	24.3	1.6
6	0.30	10	94.1	5.2	2.2
7	0.30	30	94.8	3.4	2.5
8	0.30	90	92.7	0.7	1.8
9	0.30	180	88.3	0.4	2.3
10	0.30	4320	94.8	0.0	1.7
11	0.075	90	87.9	0.0	1.3
12	0.15	90	89.4	0.1	1.8
13	0.60	90	94.9	0.0	1.9